Monatshefte für Chemie 108, 1213—1234 (1977)

Monatshefte für Chemie

© by Springer-Verlag 1977

A Constitutional Diagram of the System $VC_{0.88}$—$HfC_{0.98}$—WC

By

Peter Rogl*, Subhash K. Naik und Erwin Rudy

Materials Science Department,
Oregon Graduate Center for Study and Research,
Beaverton, Oregon, U.S.A.

With 9 Figures

(Received January 19, 1977)

The system $VC_{0.88}$—$HfC_{0.98}$—WC was investigated by means of melting point, differential-thermoanalytical, X-ray diffraction and metallographic techniques on hot pressed and heat treated as well as melted alloy specimens and a complete constitutional diagram from 1500 °C through the melting range established.

The phase behaviour within $VC_{0.88}$—$HfC_{0.98}$—WC is characterized by the presence of a large (binary) miscibility gap within VC—HfC ($T_{crit.,hypo.}$ = 3000 °C). Additions of WC decrease the miscibility gap in the ternary. Interaction of the solvus (boundary of the cubic-B1 monocarbide solution) and the ternary miscibility gap was established at 2075 °C and $(VC)_{0.17}(HfC)_{0.37}(WC)_{0.46}$: On cooling below 2075 °C alloys of this composition enter a decomposition reaction into two isotypic cubic B1 phases and hexagonal WC.

Solid state and melting behaviour was established within the isopleths $VC_{0.88}$—WC and $VC_{0.88}$—$HfC_{0.98}$ as well as within $(V_{0.8}W_{0.2})C$—$(Hf_{0.8}W_{0.2})C$ and WC—$(V_{0.38}Hf_{0.62})C$. The isopleth $VC_{0.88}$—$HfC_{0.98}$ intersects the four phase plane of the ternary V—Hf—C euctetic [2580 ± 10 °C, $(VC)_{0.78}(HfC)_{0.22}$]. Originating at the VC—HfC binary this eutetic trough proceeds into the VC—HfC—WC ternary with raising temperatures connecting the maximum critical point of the disappearing miscibility gap [$(VC)_{0.35}(HfC)_{0.51}(WC)_{0.14}$] by a limiting tie line (2830 ± 20 °C).

Isothermal sections have been calculated assuming regular solutions.

* Present address: Institute of Physical Chemistry, University of Vienna, Währinger Straße 42, A-1090 Wien, Austria.

I. Introduction and Summary of Previous Work

It was shown by *Rudy*[1] that phase stability induced critical solution phenomena offer many interesting possibilities for microstructure and property control of alloys.

With respect to development of high quality tool materials based on the principle of spinodal decomposition, a careful and basic investigation of the melting and solution behaviour among carbide systems such as WC(MoC)—TiC(VC)—HfC was planned and recently a paper was published[2] presenting a complete constitutional diagram of the TiC—HfC—WC system from 1500 °C through the melting range. The subject of the present paper was a study of the system VC—HfC—WC using the constituents at the carbon rich boundary.

Among the boundary systems of the VC—HfC—WC system the phase relationship within the isopleth HfC—WC has been well established[2].

Ettmayer[3] showed a constitutional diagram VC—HfC based on melting point observations by means of *Seger* cones as well as X-ray investigations: eutectic temperature 2650 °C at $(VC)_{0.76}(HfC)_{0.24}$.

No complete description of the isopleth VC—WC has been reported in literature. Some data on the solid solubility of the cubic (V, W)C monocarbide solution (at 1800 °C) were available from an earlier investigation of the ternary system V—W—C by *Rudy*[4]. A preliminary and more recent investigation of the ternary system V—W—C by *Rudy*[5] showed a maximum type melting point within the cubic monocarbide solution at substoichiometric compositions at $\approx$ 2850 °C, $V_{0.27}W_{0.27}C_{0.46}$.

No data on the ternary VC—HfC—WC were available in literature.

II. Experimental

Raw Materials

Monocarbide powders VC, HfC, and WC were used in preparing the experimental alloy specimens.

Vanadium monocarbide powder was purchased from Wah Chang Corporation, Albany, with an average particle size of 10 μ. The total amount of C was 17.23 wt%. Major impurities in ppm: N 40, O 1200, iron metals: 1200. The measured lattice parameter was 4.167 Å.

Tungsten monocarbide powder (Teledyne-Wah Chang-Huntsville, Huntsville, Alabama) with average particle size of 2 μ contained a total amount of carbon of 6.14 wt% C (0.02% free C); iron metal impurities were less than 0.02 wt%. The measured lattice parameters were $a = 2.905$ and $c = 2.837$ Å.

Hafnium monocarbide powder was prepared in our laboratory by reduction of HfO_2 with lampblack carbon in a carbon furnace at $\approx$ 2000 °C. The total carbon content was 49.5 at% C (0.2 wt% free C). Major impurities included 0.05 wt% N and O. The measured lattice parameter was 4.640 Å.

Sample Preparation

A detailed description of the sample preparation, melting point determination, differentio-thermoanalytical, X-ray and metallographic analysis was recently given[2] and applies as well to the present investigation.

III. Graphical Representation

Because of the substoichiometric carbon rich boundary of the monocarbide solutions and according to the carbon content of the powder materials used, the system VC—HfC—WC actually represents the concentrational section $VC_{0.88}$—$HfC_{0.98}$—WC of the quaternary system V—Hf—W—C.

In all cases if not especially denoted the symbols VC and HfC are used for the carbon saturated carbides $VC_{0.88}$ and $HfC_{0.98}$ (see also section Raw Materials).

Due to peritectic melting of WC as well as due to the melting behaviour within the binaries V—C and Hf—C at $VC_{0.88}$ and $HfC_{0.98}$ respectively, the system $VC_{0.88}$—$HfC_{0.98}$—WC is not a pseudoternary system.

As earlier discussed in case of the TiC—HfC—WC system[2] a graphical representation was used like for a true pseudoternary system: the concentrational section $VC_{0.88}$—$HfC_{0.98}$—WC as a basis and temperature as vertical axis.

But it shall be emphasized that in this type of representation the interpretation of the melting behaviour and phase behaviour is more complicated and unlike in a pseudoternary system: i.e. the liquidus surface near the WC rich corner does not represent the field of primary crystallization of WC but of carbon (Fig. 5). Similarly the $L + \delta + C$ and $L + \delta_1 + \delta_2$ phase fields do not degenerate when reaching the boundary isopleths VC—HfC, VC—WC, and HfC—WC (see also Fig. 6).

IV. Results and Discussion

The Isopleth $VC_{0.88}$—$HfC_{0.98}$

A reinvestigation of the section $VC_{0.88}$—$HfC_{0.98}$ was carried out. The boundary of the miscibility gap was established by lattice parameter evaluation at different temperatures (1500, 2050, 2580 °C; Fig. 1*a*). According to Fig. 1*a*, the mutual solubility at 2580 °C (9 mole% VC and 13 mole% HfC) is in good accordance to the values presented by *Ettmayer*[3] at his eutectic temperature (2650 °C, 9 mole% VC and 14 mole% HfC). Investigation of the high temperature behaviour within $VC_{0.88}$—$HfC_{0.98}$ revealed very sharp (eutectic) melting at 2580 ± 10 °C and $(VC)_{0.78}(HfC)_{0.22}$. This temperature is lower than the eutectic temperature recorded by *Ettmayer*[3] [2650 °C, $(VC)_{0.76}(HfC)_{0.24}$] but is in better relation to the incipient melting of $VC_{0.88}$ at 2640 °C ($VC_{1.0}$: $T_m = 2635$ °C)[6]. Metallographic investigation of specimens near $(VC)_{0.78}(HfC)_{0.22}$ showed a strong tendency of the small and spherically shaped carbide particles to accumulate, indicating high surface tension.

Carbon as a phase has been omitted from the experimentally observed diagram presented in Fig. 1*b*, as the join $VC_{0.88}$—$HfC_{0.98}$ is very near the actual high carbon boundary of the monocarbide solution $(V, Hf)C_{1-x}$. Considering the phase behaviour within V—Hf—C, the

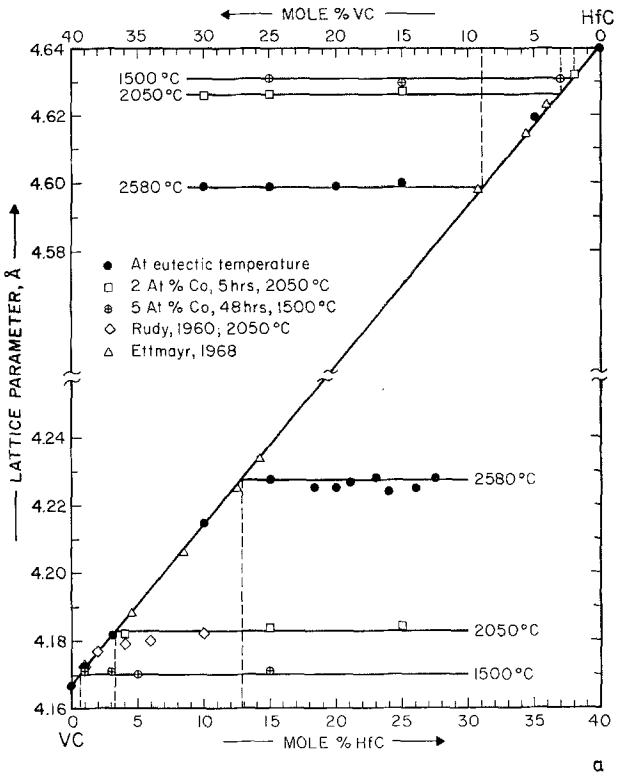

Fig. 1. *a* Lattice parameters of (V, Hf)C alloys at different temperatures

isopleth $VC_{0.88}$—$HfC_{0.98}$ just intersects the four phase reaction plane of the ternary eutectic $L \rightleftharpoons$ (V, Hf)C + (Hf, V)C + C (2580 °C, $V_{0.4}Hf_{0.1}C_{0.5}$). Therefore by a graphical solution very small and narrow phase fields $L + \delta_1 + C$, $L + \delta_2 + C$, and $L + \delta_1 + \delta_2$ appear in a complete description of the isopleth $VC_{0.88}$—$HfC_{0.98}$ as represented in Fig. 6*a*.

The Isopleth $VC_{0.88}$—WC

Solid solubility at lower temperatures was established by X-ray evaluation (Fig. 2*a*) and metallography, at higher temperatures by *DTA*.

The cubic monocarbide solution [δ-(V, W)C_{1-x}] exhibits a maximum congruent melting point (2850 °C and $V_{0.27}W_{0.27}C_{0.46}$) at substoichiometric compositions and by this a pseudobinary eutectic: $L \rightleftarrows \rightleftarrows$ (V, W)C + C. The melting and phase behaviour within the iso-

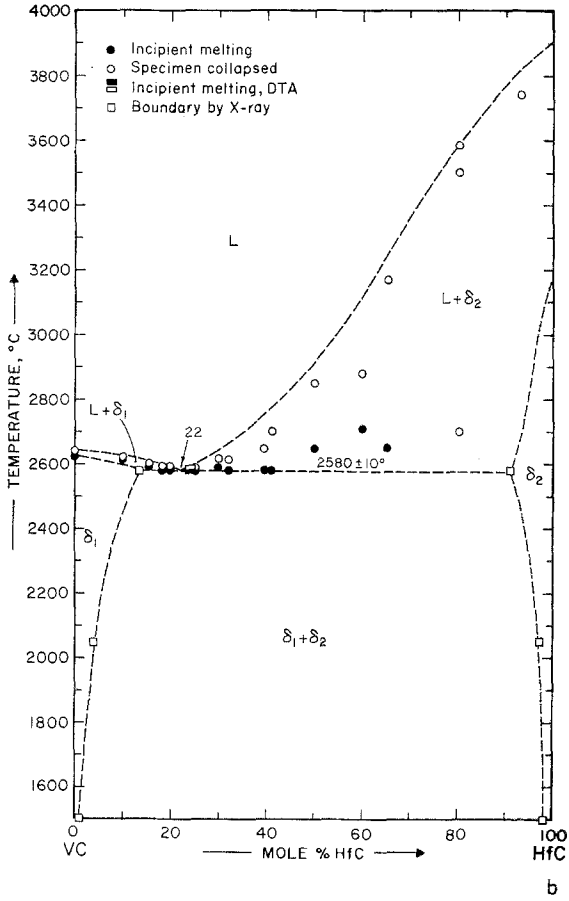

Fig. 1. *b* Experimental melting temperatures and phase distribution along the join $VC_{0.88}$—$HfC_{0.98}$

pleth $VC_{0.88}$—WC (Fig. 2*b*) is therefore similar to the TiC—WC isopleth[2]. The above mentioned pseudobinary reaction shows as a degeneration of the $L + \delta + C$ phase field at $(VC)_{0.5}(WC)_{0.5}$ (Fig. 2*b*).

Phase Equilibria in the Range From 1500 to 2100 °C

Phase equilibria at 1500 °C are dominated by the existence of an extremely large ternary miscibility gap, at higher WC concentrations intersecting the solvus boundary (Fig. 3*a*, isothermal section at 1500 °C). Carbon as a phase has been omitted from the diagram as well as from all isothermal sections in the solid state region because of the very small amounts involved.

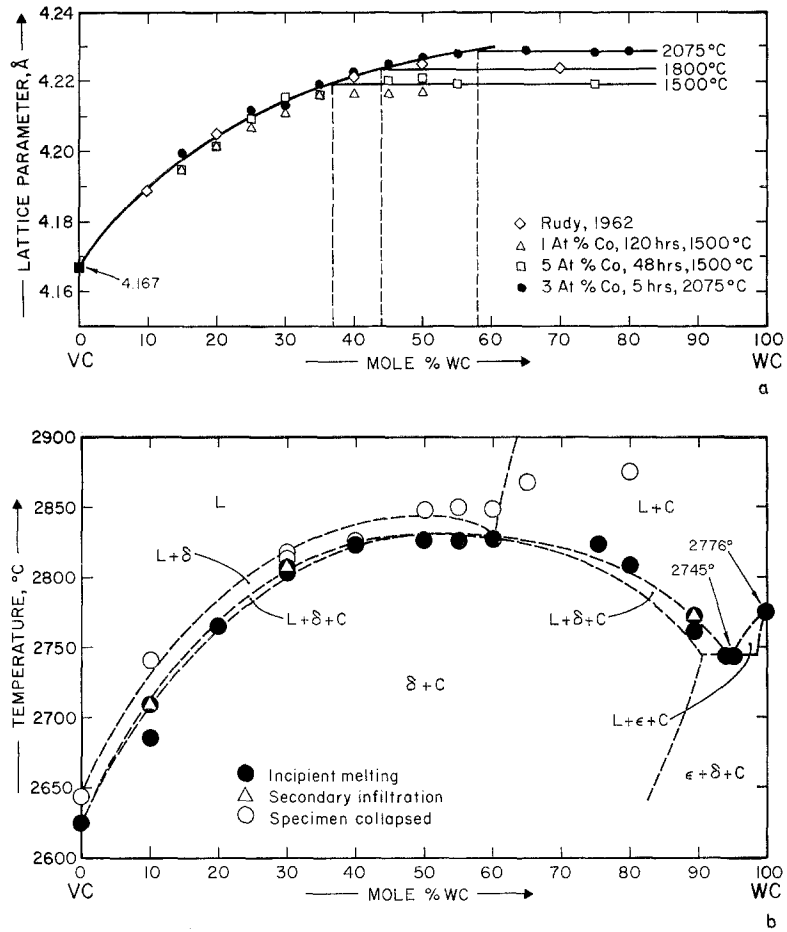

Fig. 2. *a* Location of the vertex of the three phase equilibrium (V, W)C + + WC + C at the cubic monocarbide phase by lattice parameter measurements on samples equilibrated at different temperatures. *b* Experimental melting temperatures along the join $VC_{0.88}$—WC

For an exact representation of the isothermal section at 1500 °C carbon would have to be added and furthermore very small phase fields $\varepsilon + \delta_1$, $\varepsilon + \delta_2$, and $\varepsilon + \delta_1 + \delta_2$ would appear in the very WC rich corner.

On the basis of precalculated isothermal sections (see also section V) a series of isothermal sections was studied similarly at 2000, 2050, and 2075 °C in order to localize the unique point P_c (critical point on binodal), where the miscibility gap closes and separates from the solvus. P_c: $(VC)_{0.17}(HfC)_{0.37}(WC)_{0.46}$, 2075 °C, Fig. 3*b*.

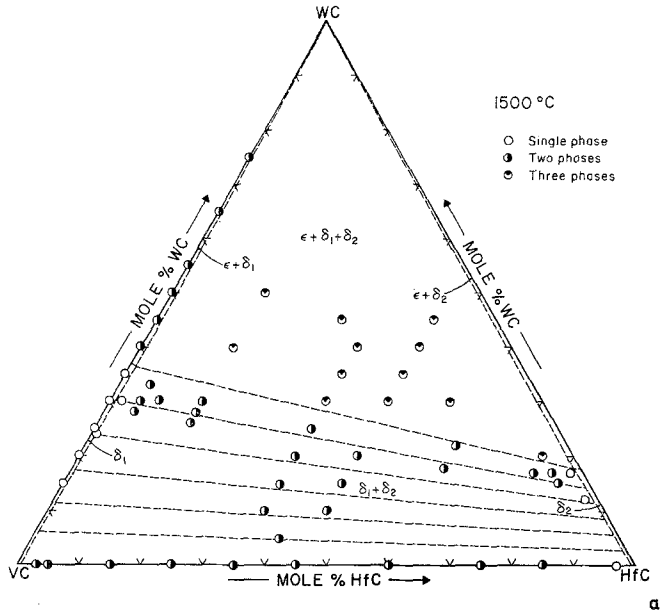

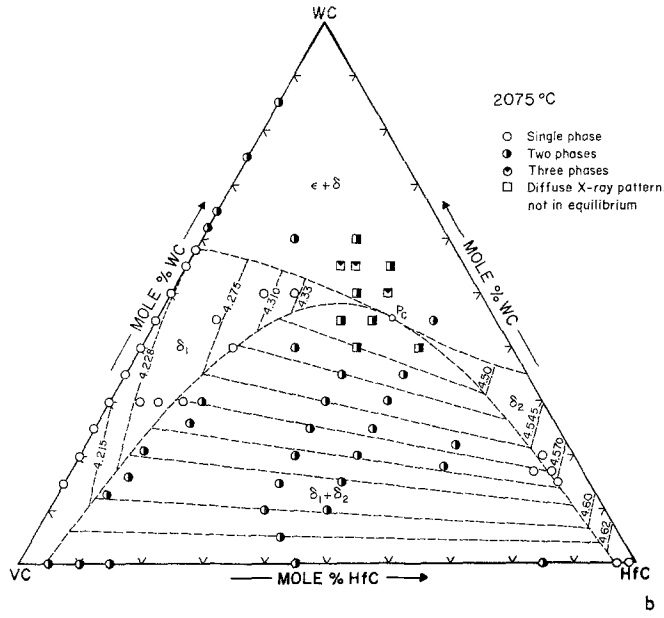

Fig. 3. Location and qualitative (X-ray) phase evaluation of alloy samples equilibrated at different temperatures: *a* 1500 °C. *b* 2075 °C

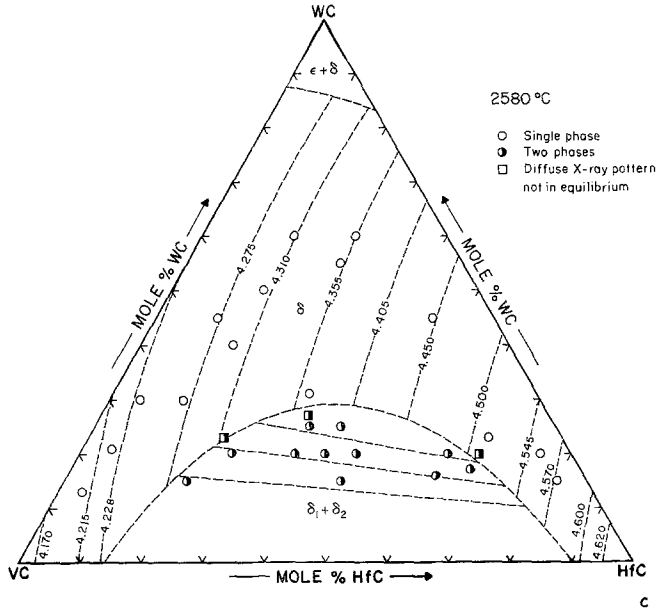

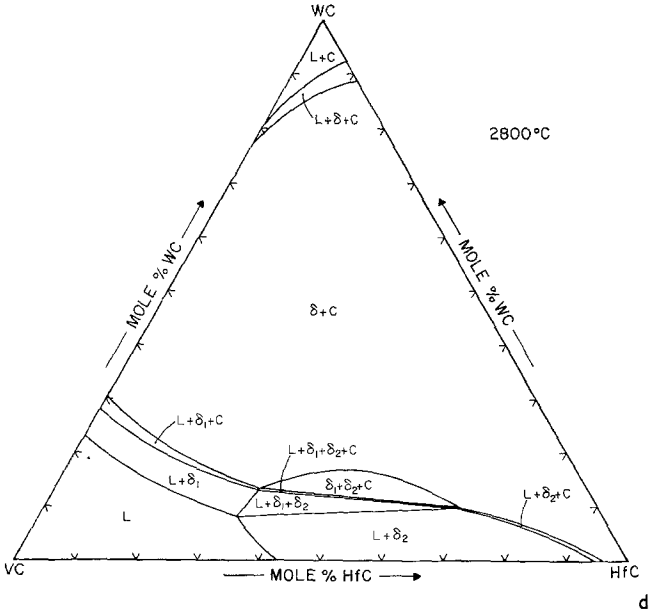

Fig. 3. *c* Location and qualitative (X-ray) phase evaluation of alloy samples equilibrated at 2580 °C, isoparametric lines. *d* Isothermal section at 2800 °C

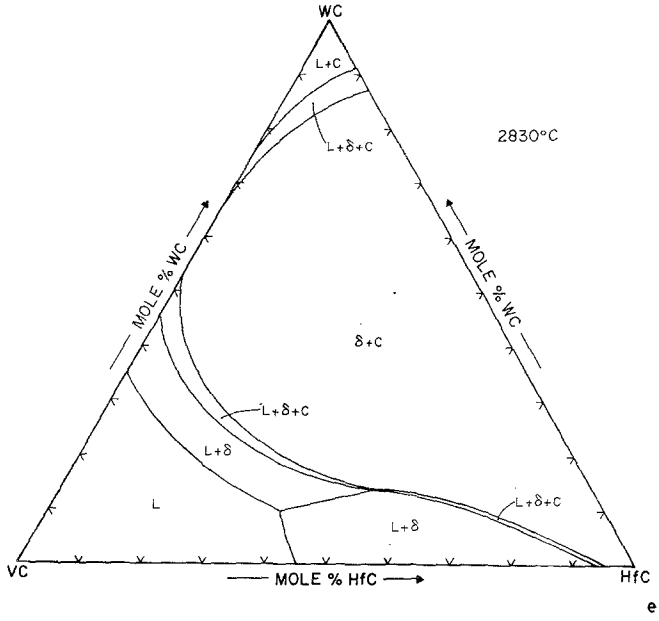

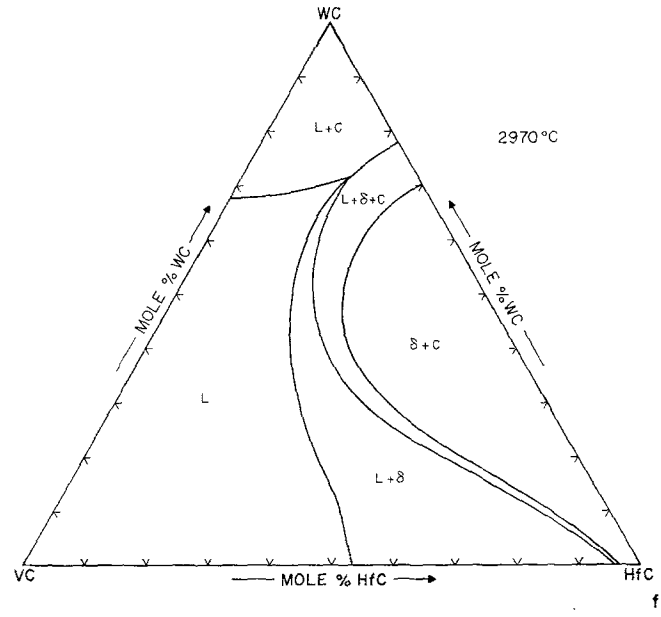

Fig. 3. Isothermal sections at different temperatures: *e* 2830 °C. *f* 2970 °C

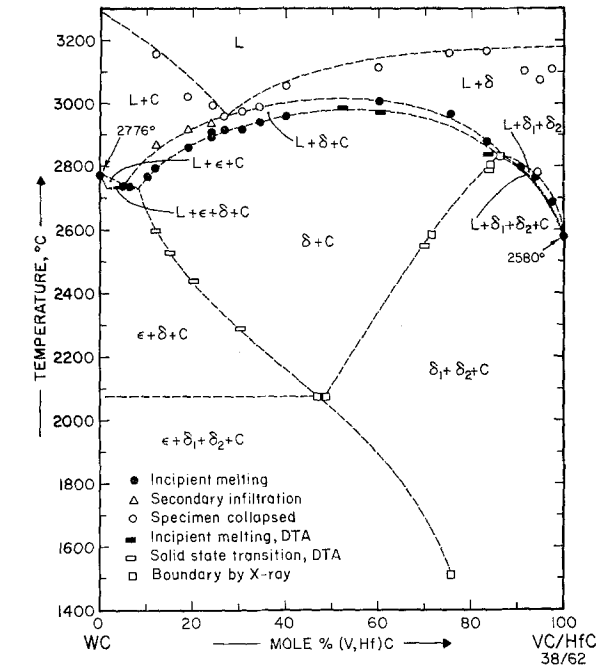

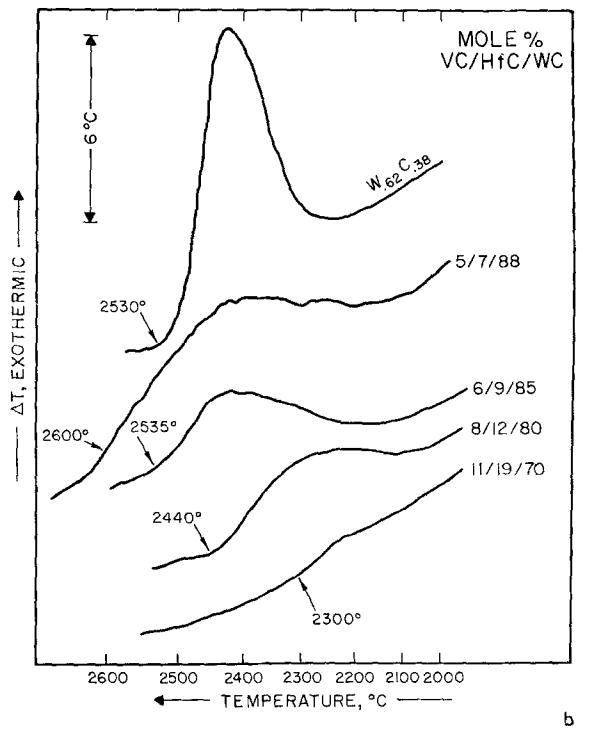

Fig. 4. *a* Melting temperatures and phase distribution along the join WC—$(V_{0.38}Hf_{0.62})C$. *b DTA* thermograms showing the disproportionation of the cubic phase in binary W—C and ternary VC—HfC—WC alloys, cooling rates at 2 °C per second

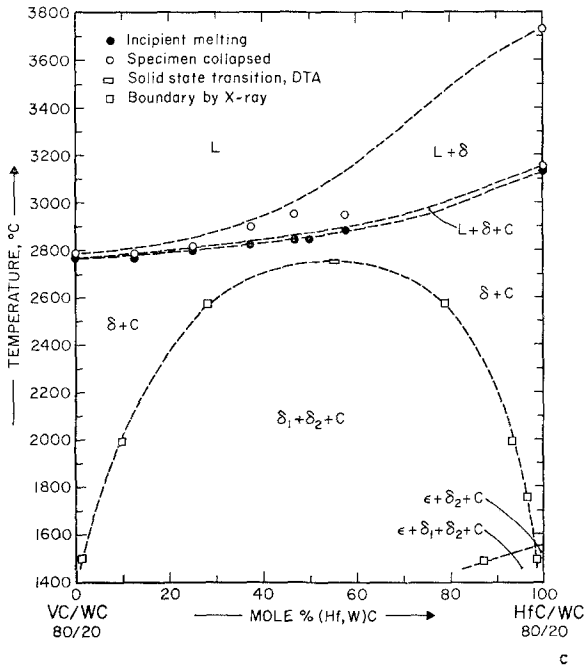

Fig. 4. *c* Melting temperatures and phase distribution along the join $(V_{0.8}W_{0.2})C$—$(Hf_{0.8}W_{0.2})C$

Below 2075° samples of composition P_c will decompose on cooling from temperatures > 2075 °C (single phase cubic) into two isotypic cubic phases (δ_1, δ_2) and hexagonal WC (ε).

The decomposition at P_c was studied on cooling in the *DTA*-apparatus, but even with extremely slow cooling rates (< 1 °C/sec) very weak signals with sloppy onset at 2000–2100 °C were obtained.

Phase Equilibria at High Temperatures

Higher temperature sections at 2580, 2800, 2830 °C have been studied in order to solve the phase behaviour arising from the interaction of the miscibility gap with the eutectic valley originating in the VC—HfC system. Heat treatment was mostly carried out in the melting point furnace and samples whenever necessary, tin quenched. Samples near the liquidus temperatures have been treated in the *DTA* apparatus because of its very stable temperature readings. Fig. 3*c* shows sample location, X-ray evaluation, isoparametric lines as well as the resulting phase behaviour in an isothermal section at 2580 °C. The higher temperature sections involving liquid as a phase have been investigated in combination with the melting point determination of solidus and liquidus surfaces.

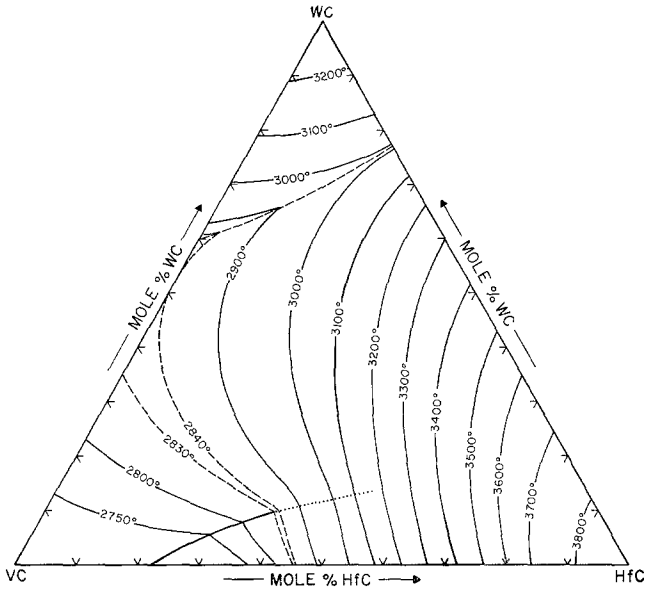

Fig. 5. Liquidus projections in the VC—HfC—WC system

According to the small amounts of carbon involved in the phase equilibria (i.e. because of the vicinity of the high carbon boundary of the monocarbide solution) the $L + \delta_1 + C$, $L + \delta_2 + C$ as well as $L + \delta_1 + \delta_2 + C$ phase fields become extremely small ($L + \delta_1 + \delta_2 + C$ degenerates into the eutectic line within the VC—HfC binary) and will disappear if the VC—HfC—WC system would be considered at the carbon rich boundary of the binaries (Fig. 3*d*, isothermal section at 2800 °C). At slightly higher temperatures 2830 °C (Fig. 3*e*) the three phase field $L + \delta_1 + \delta_2$ degenerates into a limiting tie line as well as the $L + \delta_1 + \delta_2 + C$ field degenerates almost into a point, thus the tie line connects the eutectic trough with the maximum critical point of the disappearing miscibility gap: $(VC)_{0.35}(HfC)_{0.51}(WC)_{0.14}$. At the carbon rich boundary the $L + \delta + C$ fields would degenerate too and in this case of a mixed nodal junction II + IV three lines would be allowed to meet at one point (maximum critical point) in a two dimensional diagram of 3 components[7].

The Isopleth WC—$(VC)_{0.38}(HfC)_{0.62}$

The isopleth WC—$(VC)_{0.38}(HfC)_{0.62}$ crosses the composition of the maximum critical point of the disappearing miscibility gap: $(VC)_{0.36}(HfC)_{0.51}(WC)_{0.14}$; the resulting phase behaviour is shown in Fig. 4*a*.

A more detailed consideration shows that at the carbon rich boundary the very narrow $L + \delta_1 + \delta_2 + C$ phase field will degenerate into a line and with critical elements involved 5 lines will be allowed to meet at the maximum critical point in a two dimensional diagram (3 components)[7].

Fig. 4*b* shows for some samples in the WC rich corner *DTA* thermograms on cooling (2 °C/sec). The peaks are generated on crossing the phase boundary by decomposition of the cubic monocarbide solution and rejection of hex. WC. The decomposition is very fast with sharp onset of the peaks at high WC concentrations but becomes very sluggish with sloppy peaks at lower WC concentrations. For comparison the *DTA* signal of the decomposition of cubic $W_{0.62}C_{0.38}$ is shown.

The Isopleth $(VC)_{0.8}(WC)_{0.2}$—$(HfC)_{0.8}(WC)_{0.2}$

The presented isopleth $(VC)_{0.8}(WC)_{0.2}$—$(HfC)_{0.8}(WC)_{0.2}$ (Fig. 4*c*) can be considered as a good example of the interaction of a wide miscibility gap with a two phase field $L + \delta$ (and a small $L + \delta + C$ field) in order to generate eutectic phase behaviour.

Approximately 75 alloy specimens were investigated in the melting point furnace in order to determine the liquidus as well as solidus surface within the system $VC_{0.88}$—$HfC_{0.98}$—WC (Fig. 5). The liquidus projection is characterized by the above described interaction of the VC—HfC eutectic with the maximum type miscibility gap (the limiting tie line at 2830 °C is represented by dots) and a melting trough in the WC corner: Originating at the metal—carbon binaries V—C and Hf—C[6] the monocarbide—carbon eutectic proceeds as a bivariant reaction into the ternaries V—W—C and Hf—W—C. Both eutectic valleys intersect the isopleths $VC_{0.88}$—WC as well as HfC—WC, thus creating a melting trough within $VC_{0.88}$—$HfC_{0.98}$—WC. The bottom line of this melting trough is represented by a dashed line near the WC corner (Fig. 5). Furthermore the dashed line separates the $L + \delta$ and $L + C$ field of primary cristallization (see also section III).

Assembly of the Phase Diagram

All available experimental data were combined to construct a phase diagram of the $VC_{0.88}$—$HfC_{0.98}$—WC system. For a convenient use of the constitutional diagram a number of concentration and temperature sections is shown in Figs. 3*a* through 6*c*. A three dimensional space model is presented in Fig. 7.

V. Thermodynamic Calculations

Meijering[8] extensively studied segregation in ternary regular solutions and developed the formalism for a complete thermodynamic

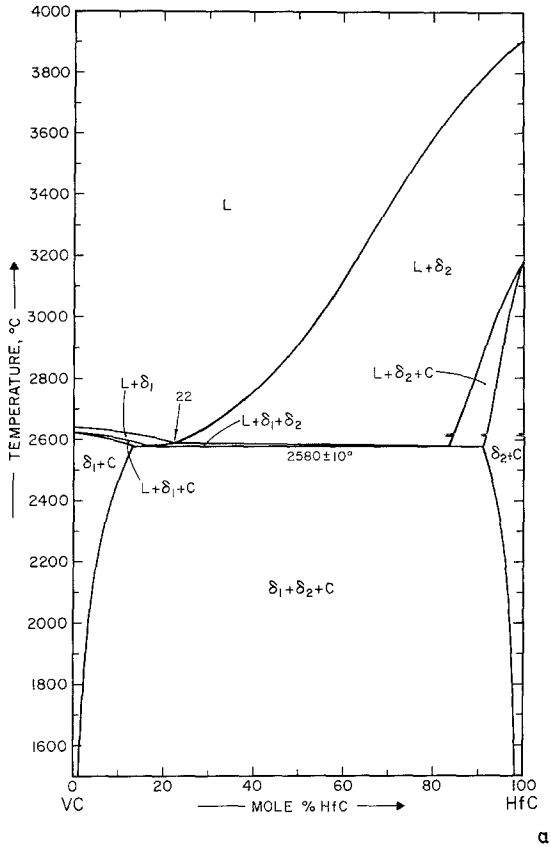

Fig. 6. *a* Isopleth $VC_{0.88}$—$HfC_{0.98}$

description. Very satisfactory results were obtained in a calculation of the ternary Ni—Cr—Cu system[9] (spinodal—solvus interaction). Very recently the regular solution approach was employed with fairly good success in calculations and precalculations of isothermal sections of the TiC—HfC—WC system[2]. In case of the almost symmetric miscibility gap of the VC—HfC system the regular solution model seems to be even more applicable.

The interaction parameters (ε, cal/mole) of the binary solutions have been evaluated by the slope of the experimentally observed tie lines across the miscibility gap, the slope of the tangent at the solvus—binodal contact point (2075 °C) as well as from the phase behaviour of the binary systems [i.e. maximum melting point of the (V, W)C solid solution at substoichiometric compositions] and a critical evaluation of ternary metal—metal—carbon equilibria.

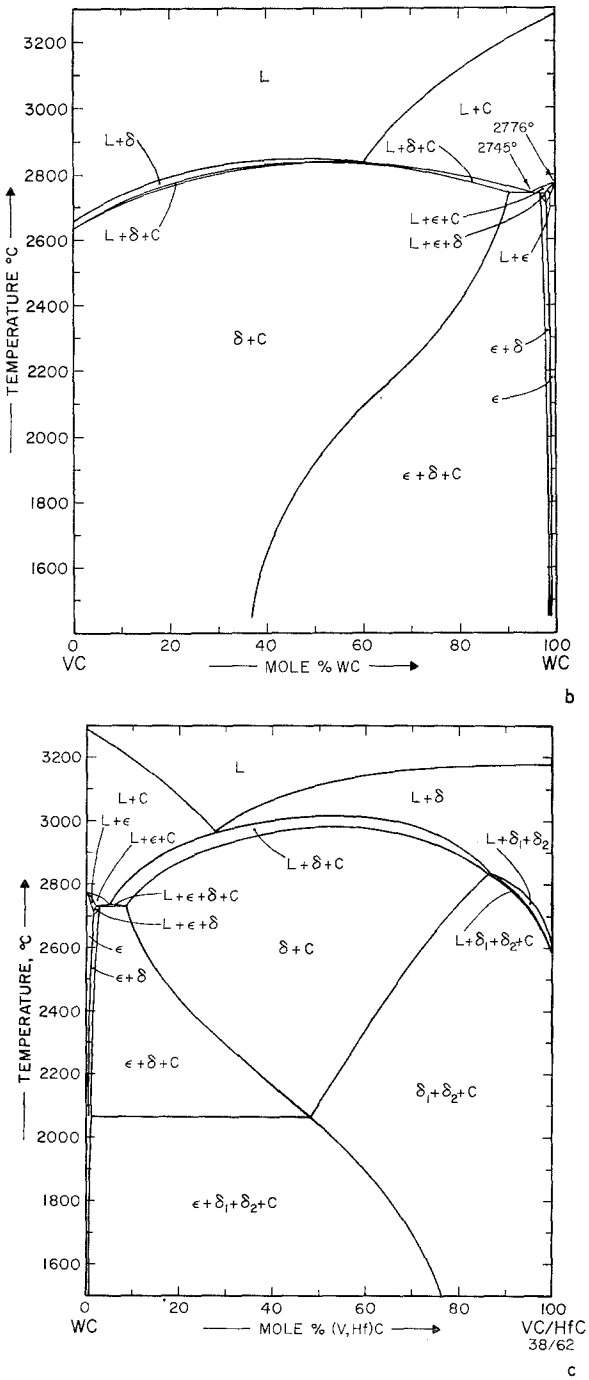

Fig. 6. *b* Isopleth $VC_{0.88}$—WC. *c* Isopleth WC—$(V_{0.38}Hf_{0.62})C$

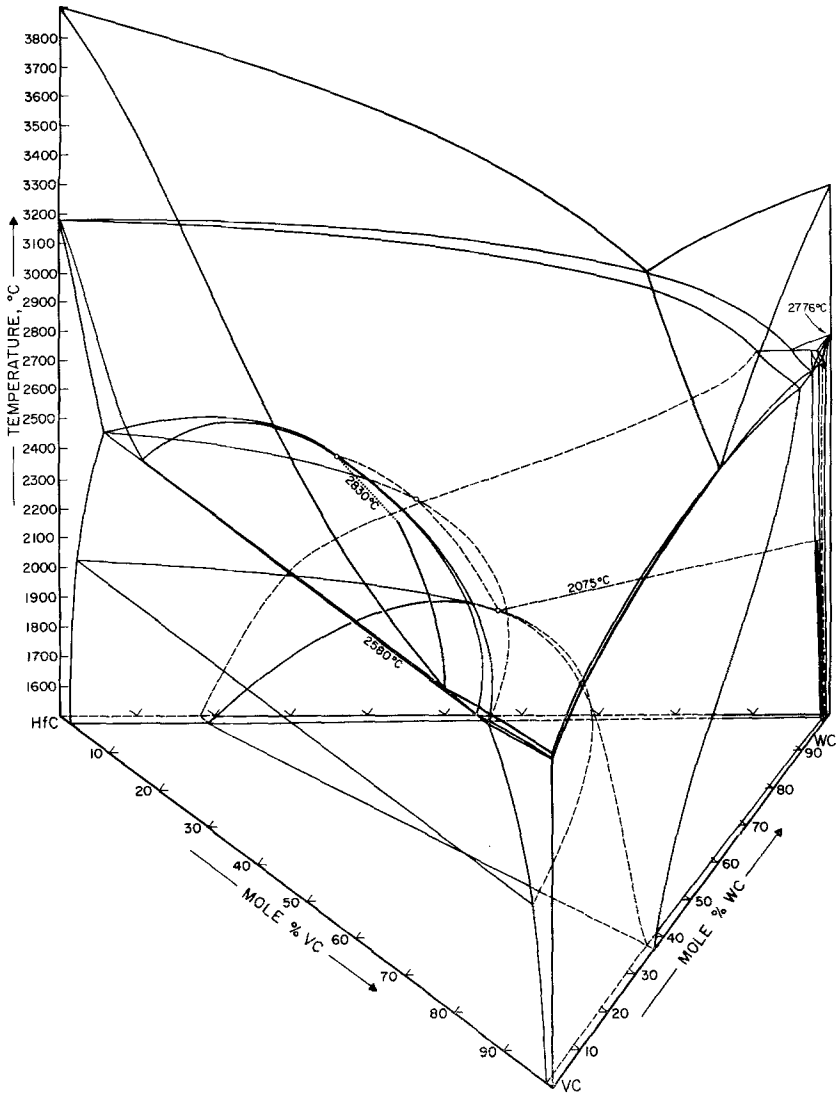

Fig. 7. Space model of $VC_{0.88}$—$HfC_{0.98}$—WC

The interaction parameter of the VC—HfC system was derived from the experimentally observed boundary of the binary as well as ternary miscibility gap in combination with a critical evaluation of the slope of the tie lines at different temperatures. In order to describe the experimentally observed phase behaviour at low as well as higher temperatures the interaction parameter $\varepsilon_{VC,\,HfC}$ had to be taken

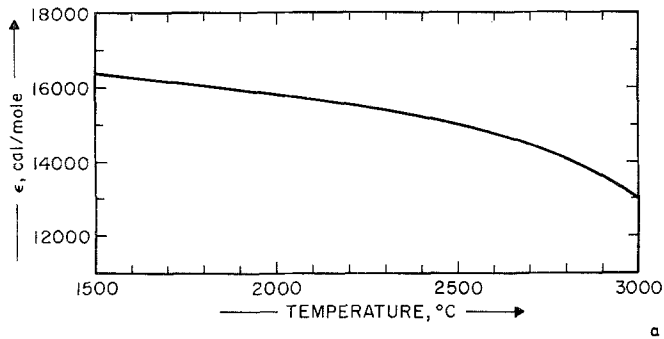

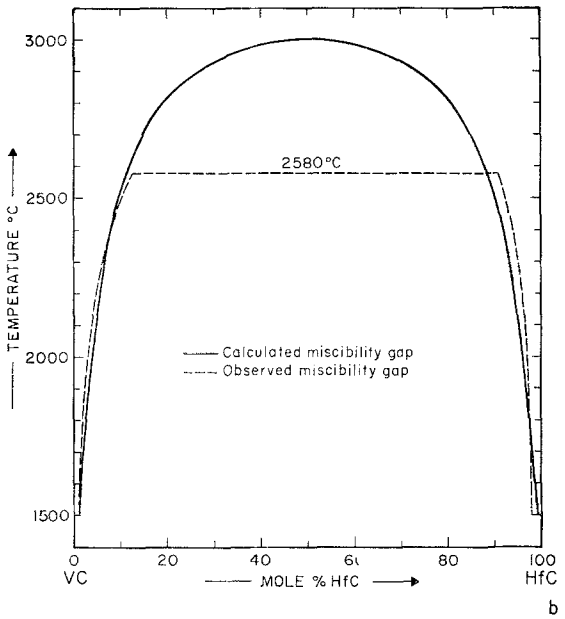

Fig. 8. *a* Temperature dependency of the regular solution interaction parameter ε of the VC—HfC system. *b* Comparison between observed and calculated miscibility gap in the system VC—HfC, regular solution

temperature dependent with decreasing values at higher temperatures.

According to this temperature dependency of ε_{VC-HfC} (see Fig. 8*a*) the hypothetical critical point of the binary miscibility gap in VC—HfC is calculated at 3000 °C, $(V_{0.5}Hf_{0.5})C$. A comparison between observed and calculated miscibility gap is shown in Fig. 8*b*. (Note: there is only a slight asymmetry in the observed miscibility gap.)

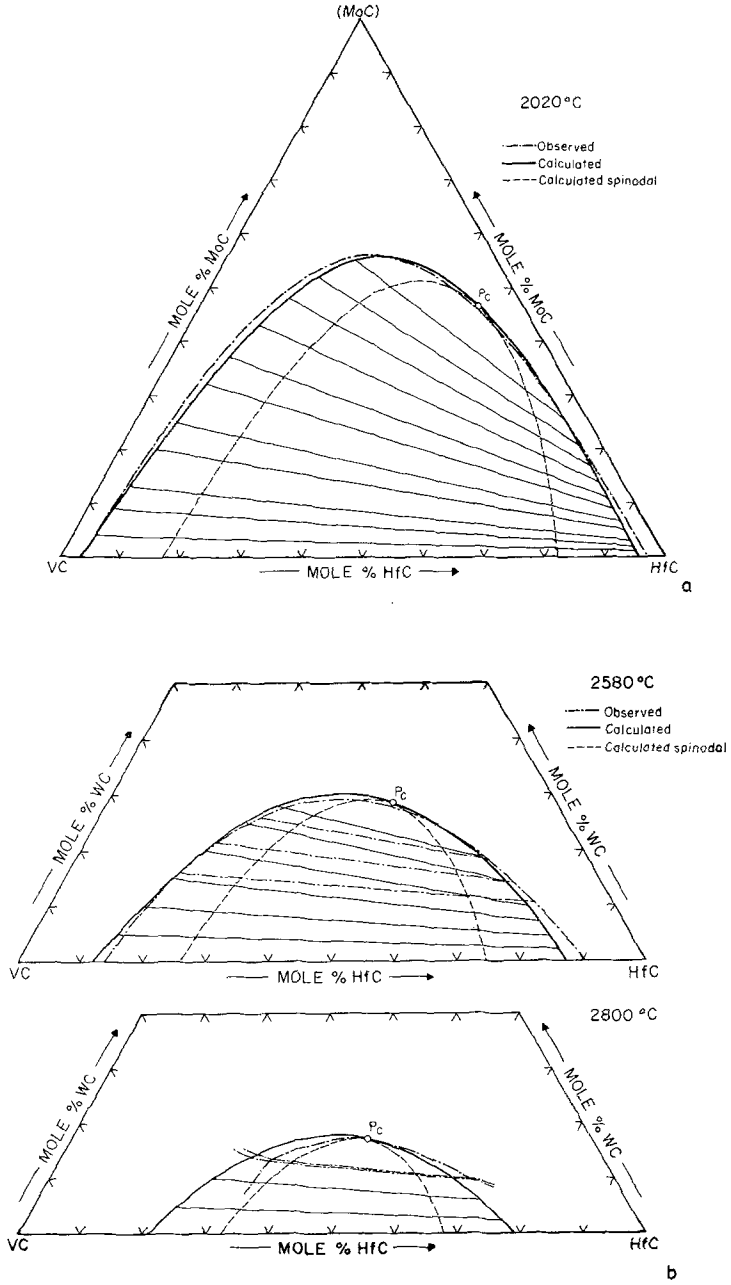

Fig. 9. Comparison between observed and calculated isothermal section of the system VC—HfC—WC at 1500 °C (*a*); at 2580 and 2800 °C (*b*)

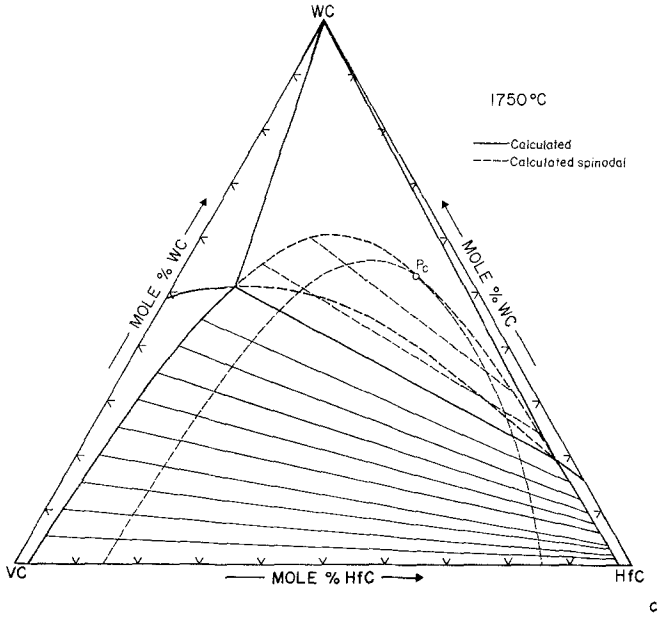

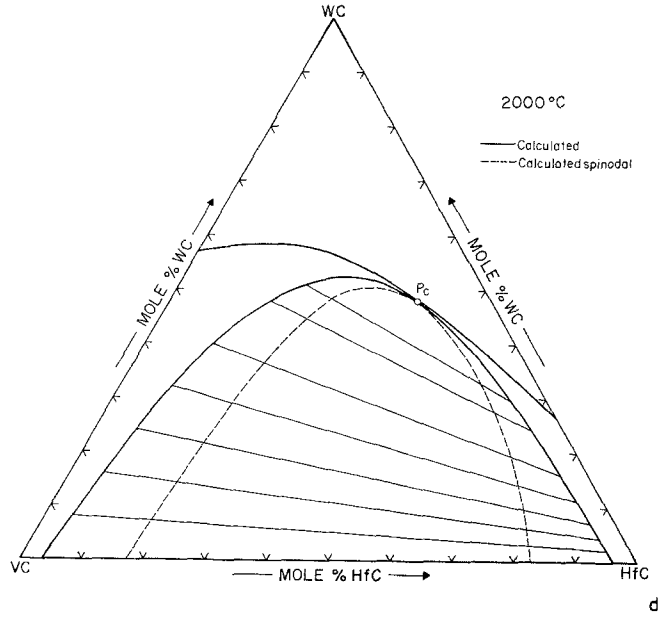

Fig. 9. *c* Calculated isothermal sections at 1750 °C; *d* at 2000 °C

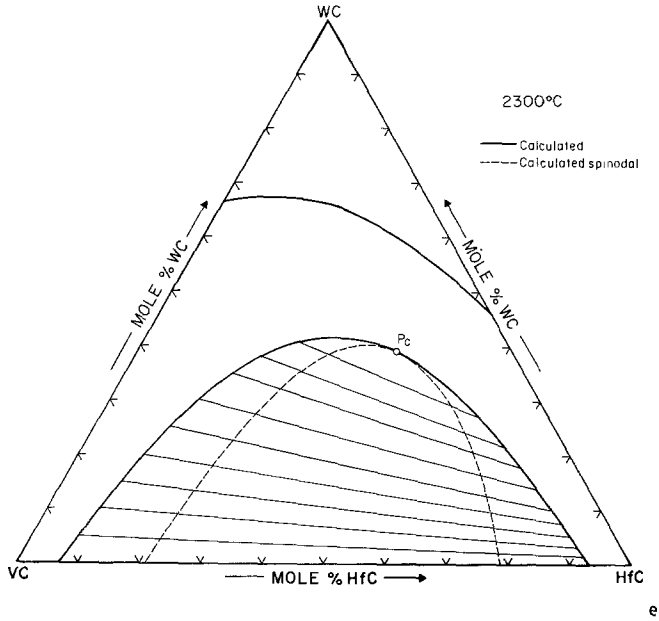

Fig. 9. *e* Calculated isothermal section at 2300 °C

The interaction parameter of the HfC—WC solution was used from an earlier calculation of the TiC—HfC—WC system[2].

The transformation energy of hexagonal WC → cubic WC at stoichiometric compositions was averaged from the observed solid solubilities of WC in VC and HfC at different temperatures and it

Table 1

ε (cal/mole)		$\Delta F_{\text{cub}\rightleftarrows\text{hex}}$ (cal/mole)	
VC—WC	−2200	TiC	20,000
HfC—WC	5500	HfC	20,000
		WC	7,800 + 2.15 T (1500–2200 °C)

was found to be of a good description in using the values derived for the TiC—HfC—WC system[2] (linear temperature dependency 1500 to 2200 °C, Table 1). The very low (practically zero at 1500 °C) solubility

of VC and HfC in WC allowed the transformation energies of VC, HfC to be taken constant within the considered temperature range (1500–2200 °C) (Table 1).

All calculations were carried out by a computer program which was established for that reason and written in FORTRAN II. It calculates the ternary spinodal, binodal, the critical point and gives the tie lines across the miscibility gap as well as the slopes of the tangents on the binodal arising from the binary gap as well as the slope of the tangent at the critical point; the program furthermore examines the possibility of a ternary saddle point or a ternary isolated critical point. A second part of the program calculates the ternary solvus curve [according to the transformation energies of the constituents]. The binodal, solvus and critical point calculations were carried out by using the *Newton—Raphson* iteration method. A detailed description of the computer program will be published[10].

Fig. 9*a* shows a comparison between the calculated and observed phase equilibria in an isothermal section of VC—HfC—WC at 1500 °C. Observation and calculation are in good agreement considering the fact that the regular solution model is a one parameter approach only. Higher temperature sections have been precalculated in order to locate the binodal—solvus interaction point and are shown at 1750, 2000, and 2300 °C (Figs. 9*c*, *d*, *e*).

Observation and calculation are in fairly good agreement [calculated critical interaction point 2000 °C, $(VC)_{0.12}(HfC)_{0.40}(WC)_{0.48}$; observed interaction point 2075 °C, $(VC)_{0.17}(HfC)_{0.37}(WC)_{0.46}$]. Higher temperature sections (Fig. 9*b*) compare observed and calculated phase behaviour at 2580 and 2800 °C and show excellent agreement concerning the slope of the tie lines as well as boundary of the miscibility gap. The second branch of the solvus (boundary of the $\varepsilon + \delta$ field in the very WC corner) is not shown in the drawings because of the very limited solid solution of the hexagonal WC even at high temperatures (< 1 mole %).

Considering the good agreement between the observed and calculated sections the very simple regular solution model approach proves to be very useful in the precalculation of uninvestigated "pseudoternary" sections as long as the regular solution interaction parameters of the binary boundary systems are known with certain accuracy; it should be noted to that point that the values of the interaction parameters (see Table 1) used in our calculations are in excellent agreement with values formerly derived by *Rudy*[11]. Furthermore it shows that precalculations will be of great value in selecting proper systems for high quality cutting tool development, based on the principle of spinodal decomposition.

Acknowledgment

One of the authors, *P. R.*, wants to express his gratitude to Prof. *H. Nowotny* (Institute of Physical Chemistry, University of Vienna) for valuable criticism and fruitful discussions.

Research sponsored by National Science Foundation grant DMR-74-23256 and by a grant by General Electric Company and Teledyne, Inc.

References

[1] *E. Rudy*, J. Less Common Metals **33**, 43 (1973).
[2] *P. Rogl, S. Naik*, and *E. Rudy*, Mh. Chem. **108**, 1190.
[3] *P. Ettmayer, R. Kieffer*, and *L. Usner*, Planseeber. Pulvermet. **16**, 108 (1968).
[4] *E. Rudy, F. Benesovsky*, and *E. Rudy*, Mh. Chem. **93**, 693 (1962).
[5] *E. Rudy*, unpublished results.
[6] *E. Rudy*, Compendium of Phase Diagram Data, AFML-TR-65-2-5, 1969.
[7] *L. S. Palatnik* and *A. I. Landau*, Phase Equilibria in Multicomponent Systems. Holt, Rinehardt and Winston Inc. 1964.
[8] *J. Meijering*, The Physical Chemistry of Metallic Solutions and Intermetallic Compounds, Nat. Phys. Sympos. HMSO, London, 1958.
[9] *J. Meijering*, Acta Met. **5**, 257 (1957).
[10] *P. Rogl*, to be published.
[11] *E. Rudy*, J. Less Common Metals **33**, 245 (1973).

Correspondence and reprints:
Dr. P. Rogl
Institut für Physikalische Chemie
Universität Wien
Währinger Straße 42
A-1090 Wien
Austria